

**Mouse Polyomavirus T Antigens: Directors of Cell Cycle Signaling**

***Catherine Nicholas***

University of Colorado, Boulder

College of Arts and Sciences

Department of Molecular, Cellular, and Developmental Biology

Defended: April 2, 2015

***Honors Thesis Advisor:***

Robert Garcea MD | Department of Molecular, Cellular, and Developmental Biology

***Honors Defense Committee Members:***

Christy Fillman PhD | Department of Molecular, Cellular, and Developmental Biology

James Goodrich PhD | Department of Chemistry and Biochemistry

Dylan Taatjes PhD | Department of Chemistry and Biochemistry

**Abbreviations**

PyV	Polyomavirus
MPyV	Mouse Polyomavirus
HPyV	Human Polyomavirus
dsDNA	double-stranded DNA
vDNA	viral DNA
UI	Uninfected
WT	Wild Type (NG59RA)
MEF	Murine Embryonic Fibroblast
hpi	Hours Post Infection
kb	kilobases
S#	Serine amino acid residue #
T#	Threonine amino acid residue #
DDR	DNA Damage Repair

**Proteins of Interest**

TAg	Tumor Antigen (L - Large, m - middle, s - small)
MRN	Mre11   Rad50   Nbs1 (protein complex)
ATM	Ataxia Telangiectasia Mutated kinase
PI3K	Phosphoinositide 3-kinase
Akt	aka Protein Kinase B; serine-threonine kinase
TOR	Target of Rapamycin; serine threonine kinase
PRAS40	Proline-rich AKT1 substrate 1; inhibitor of mTORC1
p70 S6 Kinase	Ribosomal protein S6 kinase beta-1; serine threonine kinase
p27	Cyclin-dependent kinase inhibitor 1B (p27 <sup>Kip1</sup> )

**Table of Contents**

I.	Abstract.....	4
II.	Background.....	5
III.	Aims.....	12
IV.	Materials and Methods.....	13
V.	Results.....	16
VI.	Discussion.....	24
VII.	Appendix.....	28
VIII.	Acknowledgments.....	31
IX.	References.....	32

## I. Abstract

Greater than 80% of adults are infected by one or more human polyomaviruses (HPyVs) (Kean and Garcea 2009). Polyomaviruses (PyVs) typically cause an asymptomatic infection within their hosts (birds, rodents, primates); however, under immunocompromised conditions PyV replication can cause a variety of illnesses (Fanning E. et. al. 2009). PPyV efficiently replicate by disrupting host cell signaling pathways. Disruption of the cell cycle is implicated in nearly all tumor formation. Studies of cellular transformation by primate PyV, SV40, and mouse polyomavirus (MPyV) have led to numerous findings concerning tumor suppressor proteins and cell cycle regulation pathways (Das D. and Imperiale 2009, Dahl et. al. 2005). Successful PyV replication can occur when the cell is promoted to S phase and kept there by the cell's own regulatory system. Expression of PyV T Antigen (TAg) early genes modifies signaling pathways and cell cycle checkpoints to the virus' advantage. Expected modifications include inhibiting checkpoint proteins between G1 and S phases as well as promoting kinases with downstream signaling effects that result in progression to S phase (Fanning et. al. 2009). Unlike in SV40 (Zhao et. al. 2008), the MRN complex has not been found to decrease during infection with MPyV. Other cell cycle signaling pathways are dysregulated during MPyV infection through phosphorylation events. MPyV TAg splice variants each play independent yet complementary roles in promoting viral replication. The presence of mTAg alone has been shown to alter the downstream effects of Akt and TOR pathways in order to initiate cell proliferation and push the cell into S phase, aiding viral replication (Summers et. al. 1998 and Meili et. al. 1998). Presented here is evidence of mTAg activating Akt and TOR in the context of a full MPyV infection. Furthermore, p70 S6 Kinase, a downstream effector of the Akt/TOR pathways and a motivator of translation, was also observed to increase levels of activation during MPyV infection. The cell cycle checkpoint regulator p27 was found to be suppressed during MPyV

infection, allowing the cell to progress to the S phase. MPyV mTAg is necessary, in tandem with LTag to alter cell cycle signaling that allows vDNA replication to proceed efficiently.

## II. Background

### Polyomaviridae

Polyoma describes a family of viruses that were originally named based on the observation that they can cause many (“poly”) tumors (“oma”) after injection into newborn mice. PyVs are non-enveloped, ~5-6 kb, double-stranded DNA (dsDNA) viruses. The genome encodes three early expressed genes that produce Large (L), middle (m), and small (s) TAg via alternative splicing and three late expressed genes VP1, 2, and 3 (Fig. 1). VP1, 2, and 3 are coat proteins that encapsidate the viral genome (Fluck and Schaffhausen 2009). Cell entry is facilitated by coat proteins binding to specific extracellular ganglioside receptors. Endocytosis delivers the viral capsids to the ER where they are partially disassembled and then redirected to the nucleus to begin replication of the viral genome (Fanning et. al. 2009).

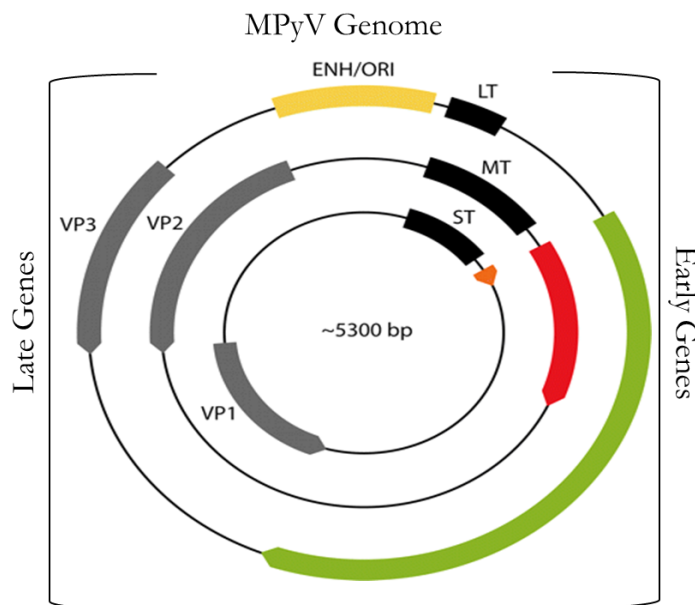


**Figure 1: Mouse Polyomavirus Genome.**

Depiction of the MPyV genome showing early genes for TAg splice variants L/m/s TAg and late genes VP1/2/3. (Adapted from Fluck and Schaffhausen 2009)

## **Polyomavirus T Antigens**

Early expression of viral TAgS is critical in driving vDNA replication. Each T antigen has a specific role in MPyV DNA replication, translation, and nascent capsid assembly. Large T antigen (LTA<sub>g</sub>) is a ~100 kDa nuclear protein with helicase activity that aids in the replication and transcription of viral DNA in addition to interacting with a wide variety of cell signaling pathways that mediate cell growth, death, and an inflammatory response. LTA<sub>g</sub> is absolutely essential for a productive PyV infection, beginning with stalling the cell in S phase and directly hijacking host replication machinery (An et. al. 2012). MPyV middle Tag (mTA<sub>g</sub>) is ~56 kDa, membrane-bound and affects numerous cell signaling pathways, viral transcription, and viral translation. In most other PyV species, only LTA<sub>g</sub> and sTA<sub>g</sub> transcripts are expressed. MPyV mTA<sub>g</sub> functions similarly to SV40 sTA<sub>g</sub>, and this gene, known as the cell transforming factor, is highly conserved in all PyVs known to date (Dilworth 2002). MPyV small Tag (sTA<sub>g</sub>), ~22 kDa localizes to the cytoplasm and is known to inhibit phosphatase 2 A (PP2A). PP2A is a tumor suppressor, and dysregulation of PP2A can result in disrupted cell signaling and transformation of the cell (Hwang et. al. 2013). Note that while each MPyV splice variant specializes in a particular aspect of infection, each likely enhances the work of the others, and together, L/m/sTA<sub>g</sub>S collaborate to drive the cell toward optimal conditions for vDNA replication and new virion assembly.

## **Mutant MPyVs**

In order to more fully appreciate the varied roles that the TAg splice variants play during MPyV infection, mutant viruses deficient in mTA<sub>g</sub> and sTA<sub>g</sub> were used and compared to the wild type (WT) virus (NG59RA). Mutant MPyVs described in the following work include NG59 and 808A (Fig 2). The NG59 mutant was selected in a chemical mutagenesis screen. NG59 has a codon insertion (ATA) immediately followed by a nucleotide change (G→A). This results in an extra

isoleucine and an amino acid change of Aspartate (negatively charged) to Asparagine (polar, uncharged) in the mTAg region (Carmichael and Benjamin 1979). These mutations reduce the normal functions of mTAg and sTAg. MPyV mutant 808A was created by site directed mutagenesis resulting in a deletion of the mTAg splice acceptor site. The deletion completely abrogates expression of mTAg while still allowing for normal LTag and sTAg expression. The WT virus used as a control was rescued from the NG59 mutant and is termed NG59RA, but will be referred to simply as RA henceforth. RA expresses fully functioning LTag, mTAg, and sTAg (Benjamin 1970, Benjamin 1982, Garcea et. al. 1989).

Immunofluorescence of infected cells shows co-localization of MPyV DNA and the proteins of the MRN complex in WT and mutant MPyV infections (Erickson et. al. 2012). However, MPyV mutant strains are impaired in their ability to replicate viral DNA and produce infectious viral progeny (Dawei 2009). Observations of mutant infections show that viral replication centers are smaller in cells infected with mTAg and sTAg deficient strains. Additionally, virus mutants unable to express mTAg and sTAg produce new virions at lower levels than WT. These data suggest that mTAg and sTAg may play a role in viral replication by regulating the MRN complex or other cell signaling activity. My work investigates the interaction of MPyV TAg with host cell signaling pathways and suggests how the absence or presence of mTAg and sTAg may affect such interactions.

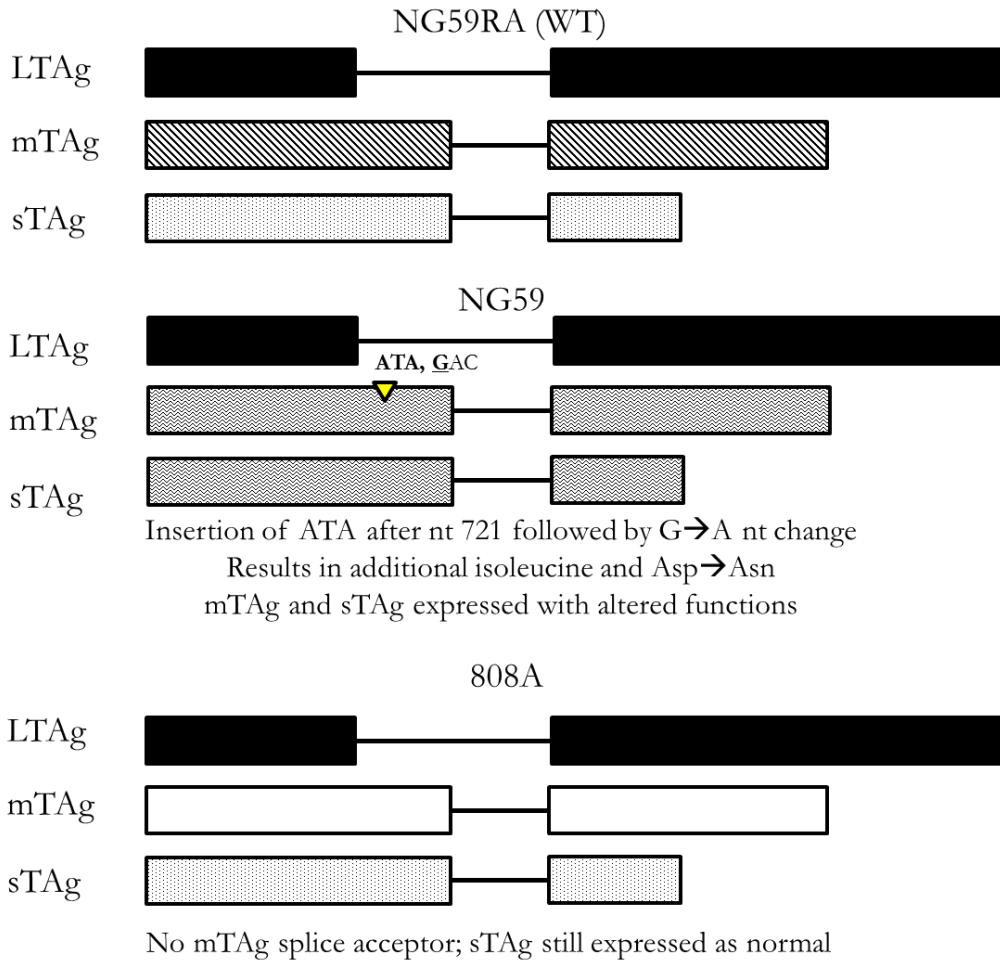
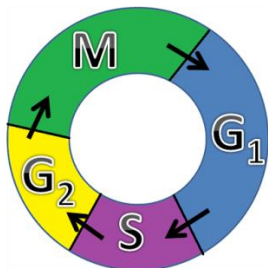


**Figure 2: Diagram of Mutant TAg.** NG59RA, NG59, and 808A MPyV TAg genes are depicted. MPyV RA expresses all three splice variants, LTAg, TAg, and sTAg. MPyV mutant NG59 expresses LTAg as normal. As indicated, the MPyV mutant NG59 has a mutation in mTAg which causes both mTAg and sTAg to have reduced functionality when expressed. MPyV mutant 808A also expresses a normal LTAg transcript as well as a normal sTAg transcript. The splice acceptor site for mTAg is deleted in mutant 808A, so no mTAg transcript is expressed.



**Cell Cycle**  
**G<sub>1</sub>: growth**  
**S: DNA synthesis**  
**G<sub>2</sub>: growth and mitosis prep**  
**M: mitosis (cell division)**

**Figure 3: Cell Cycle.** Diagram illustrating phases of the cell cycle: G<sub>1</sub>, S, G<sub>2</sub>, M. Progression between phases is regulated by checkpoint proteins and kinase activity.

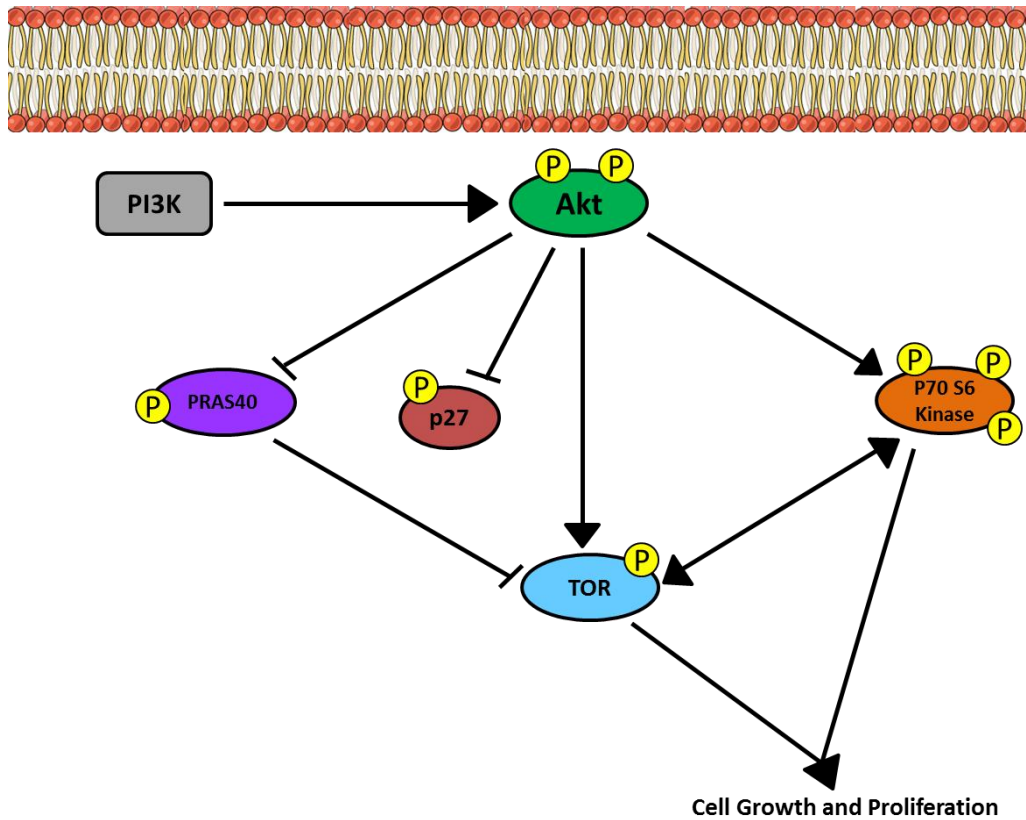


**Figure 4: Cell Proliferation Signaling.** Activation of the PI3K/Akt pathway leads to a myriad of downstream effects. Of interest in the context of this discussion is the promotion of cell growth and proliferation via translation activity through TOR and P70 S6 Kinase.

### Cell Cycle Signaling

Eukaryotic cells follow a conserved cell cycle that consists of growth ( $G_1$ ,  $G_2$ ), DNA replication and synthesis (S), and division (M – mitosis) phases (Fig. 3). Transition between phases, particularly  $G_1 \rightarrow S$  and  $G_2 \rightarrow M$ , is regulated by a variety of pathways and checkpoints. These regulatory pathways are largely activated or inhibited by kinases. The presence or absence of a phosphate group on proteins determines their activation state, interaction with other proteins, and ability to regulate downstream effectors, all of which are crucial in directing the cell cycle. It is common for transmembrane receptor proteins, often kinases, to relay signals from extracellular ligands to intracellular proteins that regulate cell cycle pathways (Diaz-Moralli et. al. 2013). PI3K, a kinase that interacts with intracellular domains of membrane proteins, phosphorylates Akt initiating

a series of downstream effects (Fig. 4). Akt (also known as Protein Kinase B) is a protein with Serine-Threonine kinase activity that directly promotes glucose metabolism, apoptosis, cell growth, transcription, and cell migration. Activation of Akt can lead to direct activation of the TOR complex. The TOR complex is negatively regulated by PRAS40. Akt has been shown to directly phosphorylate PRAS40 T246, releasing it from the TOR complex and allowing TOR to be activated. Additionally, Akt has been shown to phosphorylate and activate the TOR complex. Upon TOR activation, activities such as amino acid biosynthesis, translation, and cell proliferation are promoted, driving the cell towards the S phase. Additionally, both Akt and TOR activate p70 S6 Kinase which is known to play a role in targeting translation machinery activation for cell proliferation (Wiza et. al. 2012). p27, a cell cycle regulator, controls progression of the cell cycle at G<sub>1</sub>. Upon phosphorylation, p27 suspension of the cell cycle is lifted and the cell progresses to S phase for DNA replication (Fujita et. al. 2003). Progression of the cell cycle into S phase is regulated by these proteins (among many others) and contributes to activation of transcriptional and translational machinery.

### **Viral Disruption of Normal Cell Cycle Signaling Pathways**

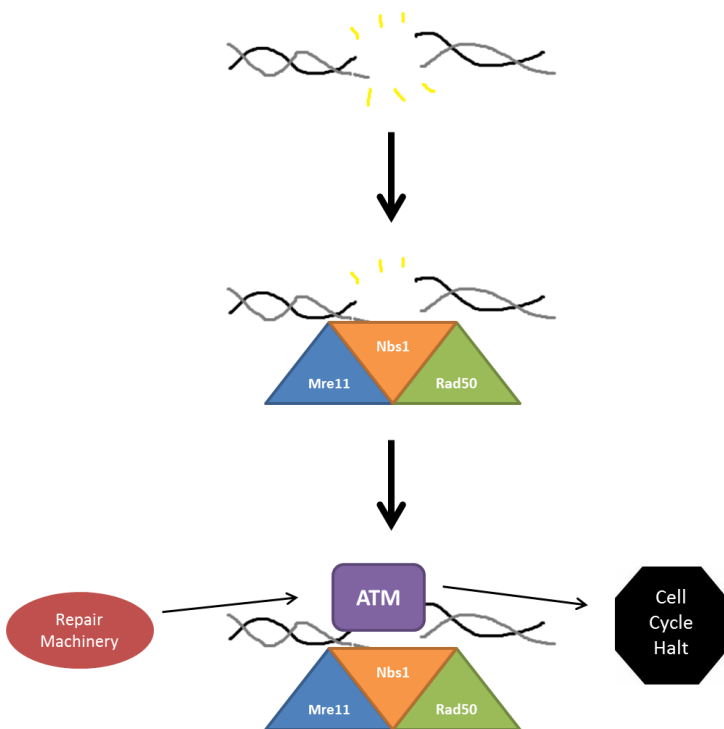
Viruses typically either evade cell cycle regulation checkpoints or commandeer them to give viral DNA (vDNA) replication priority. PyVs actively disrupt normal cell cycle signaling in order to promote efficient vDNA replication by encouraging the cell to move into S phase. PyV mediated disruption occurs via activation or inhibition of key signaling molecules that affect various regulatory mechanisms. LTA<sub>g</sub> directly binds Rb, thereby preventing Rb from halting the cell cycle at G<sub>1</sub> (Cheng 2009). MPyV mTA<sub>g</sub> serves as a membrane bound platform for various cellular factors (PP2A, c-Src, etc.) to assemble and modify signaling pathways. These modifications occur via

phosphorylation by kinases and can contribute to tumor formation by altering cell cycle signaling (Das and Imperiale 2009, Dahl et. al. 2005).

### Nuclear Cell Signaling during MPyV Infection

During events of stress or damage, the cell cycle is paused to allow time for specific repair machinery to assemble and respond to the damage. This halt of the cycle prevents damaged DNA from being replicated. Repair machinery is recruited by specialized DDR pathways which are activated as soon as damage is detected. ATM kinase (an important regulator of the cell cycle) is activated in the presence of double-stranded breaks (ionizing radiation) and halts cell cycle progression (Fig. 5). The MRN complex (Mre11, Rad50, Nbs1) is required for the recruitment of ATM kinase, leading to downstream signaling of other DDR proteins. ATM kinase induces a cell-cycle halt at  $G_1 \rightarrow S$ , intra-S, and  $G_2 \rightarrow M$  in order for repair to occur (Kurz and Miller 2004).

PyV LTA<sub>g</sub> expression results in activation of DDR pathways, specifically the ATM pathway.



In the case of PyV infection, DDR proteins are utilized to support viral replication. During PyV infection, proteins of the MRN complex are localized to sites of vDNA replication and ATM kinase is activated (Dahl et. al. 2005, Zhao et. al. 2008). Data not depicted here shows that

**Figure 5: Double-strand DNA Break Repair** The MRN complex associates with damaged DNA at the site of the break. This association recruits ATM Kinase to the site which results in bringing repair machinery in to repair damage and suspending the cell cycle until damage is repaired.

the MRN complex is chromatin associated; however, the roles of viral proteins in recruitment of the MRN complex and other DDR proteins are poorly characterized. Work from Zhao et. al. 2008 describes a proteasome dependent degradation of MRN, specifically Rad50 and Nbs1, as primate PyV SV40 infection proceeds. The authors found that ATM and MRN co-localized with viral replication centers and suggested that ATM was recruited by TAg. They propose that ATM serves as the “master regulator for TAg-directed host reprogramming” due to their published evidence that it directs the MRN complex for degradation. Evidence for TAg interaction with ATM signaling once again implies that the virus takes command and reorganizes normal cell signaling processes in order to promote efficient vDNA replication.

### **III. Aims**

**Question: How does the presence of MPyV TAg influence DDR, Cell Cycle, and Cell Signaling pathways?**

**Aim I:** Do MRN complex protein steady state levels decrease in response to MPyV infection as is reported in SV40 PyV?

**Aim II:** How does the presence or absence of TAg splice variants mTAg and sTAg in MPyV mutants affect phosphorylation of other cell signaling proteins?

#### IV. Materials and Methods

##### *Tissue Culture:*

C57 Mouse Embryonic Fibroblast C57 cells were grown in Dulbecco's Modified Eagle's Medium (DMEM, Sigma) with 10% Fetal Bovine Serum (FBS), 1% Penicillin-Streptomycin Solution (P/S), and 60 $\mu$ M  $\beta$ -Mercaptoethanol (BME). Cells were maintained in an incubator at 5% CO<sub>2</sub>, 37<sup>0</sup>C.

##### *Infection*

16-24 hours prior to infection, cells were treated with starve media (0.5% FBS/DMEM/P/S/BME). Cells were infected with NG59RA (RA), NG59 and 808A viruses (kindly provided by Tom Benjamin) in Adsorption Serum (HBSS / 0.5% BCS / 10 mM HEPES pH 5.6). After a 1.5 hour infection, the cells were placed in starve media for 24 or 26-28 hours until lysis or fixing respectively. Multiplicity of Infection (MOI) are the standard units describing the number of virus particles infecting each cell and is calculated from the titer of the virus stock and dilution required for a specific level of infection. Cells are infected with the same MOI for each experiment.

##### *Viral Infection Level Quantification Assay:*

Using a 96-well plate, 2000 cells/well were plated and infected as described above, though serial dilutions of virus were used for infection. At 26-28 hpi, cells were fixed with 4% paraformaldehyde in PBS and permeabilized with 0.5% TritonX100 in PBS. After blocking in 5% BCS/PBS serum for one hour to overnight, the cells were stained with primary antibodies TAg and VP1 for 45 minutes at 37<sup>0</sup>C. Following the primary antibodies, Rat AlexaFluor 546 and Rabbit AlexaFluor 488 secondary antibodies were applied to each well for 45 minutes at 37<sup>0</sup>C. Afterwards, 5  $\mu$ g/ml Hoechst dye was added to stain the nuclei for 15 minutes. The plate was imaged on the Molecular Devices ImageXpress Micro XL microscope using MetaXpress software with the help of Katie Heiser. Cell counts and percent infections were calculated through analysis with ImageJ.

*Cell Lysis:*

Cells were scraped into starve media and centrifuged for 10 minutes at 1500 rpm. Pellets were then washed with 1 ml ice cold PBS and then centrifuged for 5 minutes at 10,000 rpm. Pellets were lysed with 200 ul 2X SDS Lysis Buffer (25mM Tris, pH 6.8 / 1% SDS / 6.25 mM EDTA) on ice for 15 minutes. Each sample was briefly sonicated to shear DNA.

For the p-Akt/Akt immunoblots, Lysis Buffer 6 (LB6) from R&D Systems Human Phospho-Kinase Array Kit (ARY003B) was used on cells at 24 hpi. Lysis procedure was the same.

Previous work was done to optimize the lysis buffer. Lysis buffers tested include: various SDS based solutions, TEB (PBS / 0.25% TritonX100, with protease inhibitors for cytoplasmic proteins), 0.2N HCl (nuclear proteins), RIPA (50 mM Tris pH 7-8 / 150 mM NaCl, 0.1% SDS / 0.5% sodium deoxycholate / 1% TritonX100), and CSK (10 mM PIPES pH 6.8 / 100 mM NaCl / 300 mM sucrose / 3 mM MgCl<sub>2</sub> / 1 mM EGTA / 0.5% TritonX100, with protease and phosphatase inhibitors – isolates soluble and insoluble fractions). TEB and CSK buffers confirmed that MRN was chromatin associated. The 2X SDS Lysis Buffer described was determined to produce the cleanest samples for immunoblotting and is the buffer used for the MRN and TAg protein blots shown here.

*SDS-PAGE and Immunoblotting:*

After extraction, total protein concentration of each sample was determined by BioRad DC Protein Assay (Thermo Scientific Pierce BCA Protein Assay for lysates obtained from LB6). Samples were prepared by dilution in 4x SDS Sample Buffer (1 M Tris, pH 6.8 / 2% SDS / 12.5 mM EDTA / 40% Glycerol / 600 mM BME / 0.02% Bromophenol Blue) and boiled. After, samples were loaded on 8% PAGE gels at 50 ug/ul (15 ug/ul for LB6). Proteins were transferred to PVDF membranes and stained with the indicated antibodies. Prior to antibody incubation, membranes were blocked in 5% milk with 1 mM Na<sub>3</sub>VO<sub>4</sub> and 25 mM NaF phosphatase inhibitors for 30 minutes to overnight.

<b>Table 1: Antibodies.</b> List of antibodies used in experiments along with their source.	
<b>Antigen</b>	<b>Antibody Source</b>
TAg	Brian Schaffhausen (PN116)
Mre11	GeneTex (GTX118741)
Rad50	GeneTex (GTX119731)
Nbs1	Novus (NBP1-06609)
Tubulin	Novus (NB120-11304) clone B-5-1-2
pAkt	Cell Signaling #4058
Akt	Cell Signaling #9272

Antibodies (Table 1) were detected with the enhanced chemiluminescence kit from Thermo Scientific and imaged or exposed to film. Observed bands were quantified by calculating the integrated density and normalizing to a tubulin loading control.

*R&D Systems Proteome Profiler Human Phospho-Kinase Array Kit*

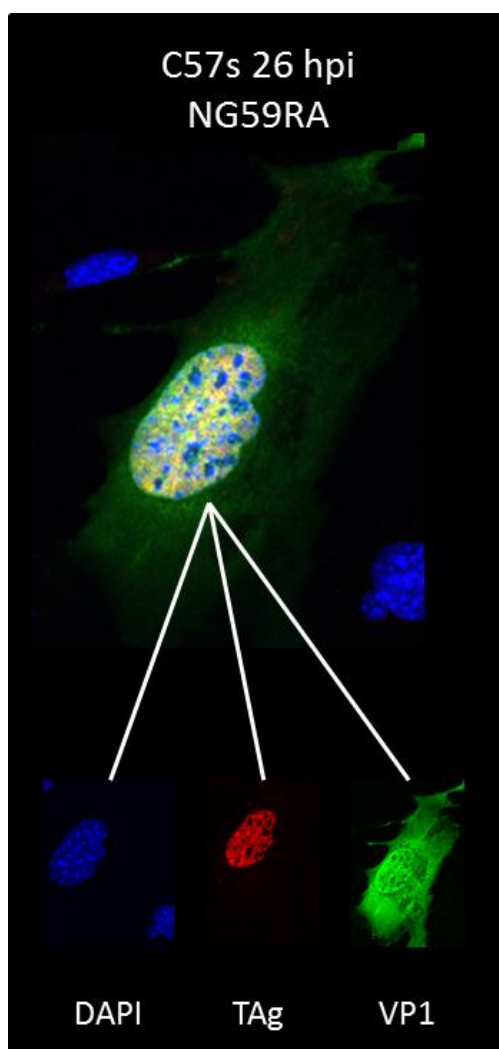
In order to identify the phosphorylation state of common cell cycle signaling kinases, a phospho-kinase array produced by R&D Systems was used. Sample lysate was applied to the provided membranes which contained antibodies specific for a variety of target proteins. Next, a second solution of antibodies were added that are specific for phosphorylation sites on the target proteins. A Biotin-Streptavidin-HRP solution was added, resulting in a chemiluminescent reaction from which the membranes can be imaged or developed. Much like an immunoblot, the resulting dots can be quantified by calculating the integrated density of each and normalizing to a PBS spot.

Sixteen 10 cm<sup>2</sup> dishes were plated with 4.8 x 10<sup>6</sup> cells/dish, two 96-well plates were plated with 2000 cells/well, and sixteen glass coverslips for confocal microscopy were plated with 1.6 x 10<sup>5</sup> cells/coverslip. All cells were infected as described above with an MOI=30. The specific dilutions used were calculated and normalized based on varying cell numbers and volume of liquid in a dish. These calculations made sure the same number of virus particles had access to each cell – ensuring sufficient levels of infection and subsequent TAg expression. Eight of the 10 cm<sup>2</sup> dishes were used for the array, while the remaining eight dishes were used to collect lysate with the Array Kit lysis buffer 6 for immunoblot analysis. The 96 well plates were used to confirm normalized levels of infection for the Array. At 24 hpi, the kit was used as directed, extra lysate was collected for immunoblots, and the 96-well plates were prepared for imaging as described previously.

## V. Results

### Viral Protein Expression during MPyV NG59RA Infection at 26 hpi Confocal Microscopy

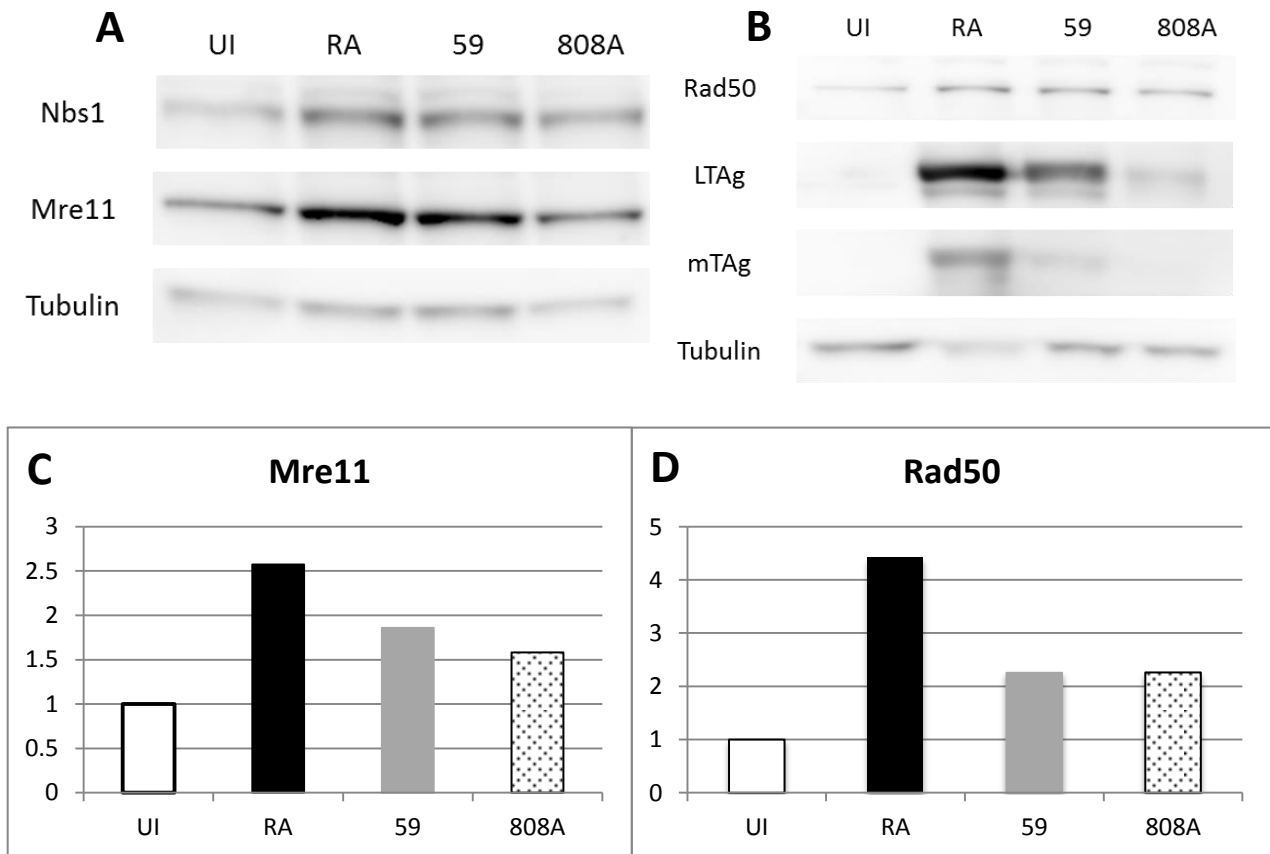
At 26 hpi with MPyV RA, the cell has begun expressing both early and late genes (Fig. 6). Expression indicates that the virus has successfully trafficked to the nucleus and was able to produce TAg. TAg expression then likely altered cell cycle regulation to promote S phase, allowing viral control of replication machinery.



**Figure 6: Expression of TAg and VP1 during infection of RA at 26 hpi.**  $1.6 \times 10^5$  C57 cells per glass coverslip were infected with RA MOI 30 as described in the methods. At 26 hpi the cells were fixed, permeabilized, and stained for TAg and VP1. Images were taken on a Nikon A1R Confocal and TIRF microscope with the help of Sam O'Hara and analyzed using ImageJ.

### MRN protein levels are not decreased during viral infection

Immunostaining for MRN proteins in samples infected with MPyVs RA, NG59, and 808A does not show a decrease in protein abundance as compared to an UI sample (Fig. 7 A, B, C, D, E). All samples were quantified and normalized to the protein loading control tubulin. The data shown are representative of 23 repeated experiments using various extraction buffers and extraction times post infection for optimization. All MRN protein immunoblot data previously compiled from the differing extraction methods concur that there is not a decrease in MRN proteins during infection by WT or mutant viruses. The change in MRN protein abundance pictured is an insignificant increase (Fig. 7 C, D, E). Immunostaining for TAg confirms that the correct virus was used for each sample and the UI sample was not contaminated (Fig. 7 B, F).



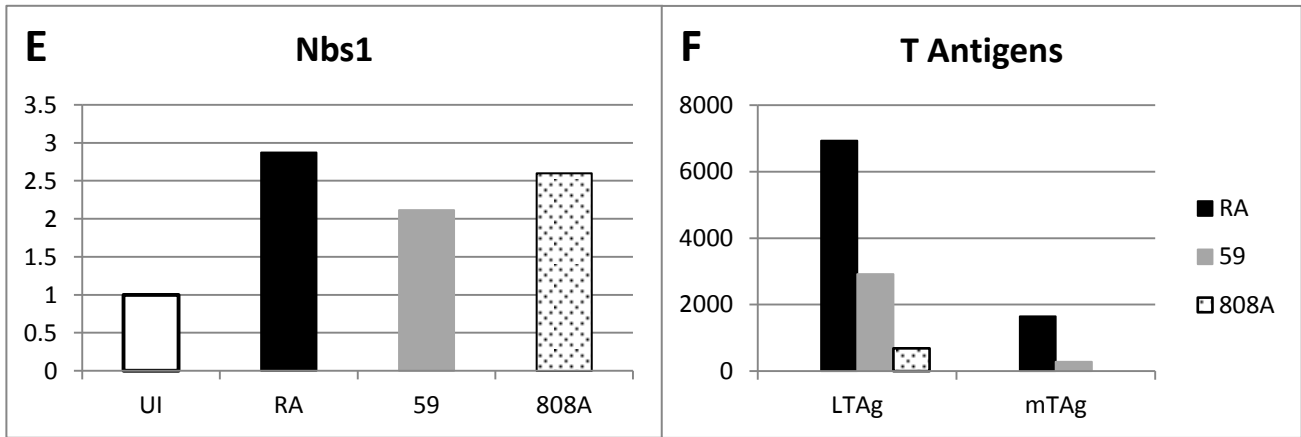


**Figure 7: Analysis of MRN expression in response to infection.** C57 MEFs were infected with MPyVs RA, NG59, and 808A (with an UI mock-infected control) for 1.5 hours. Whole cell lysates were harvested with 2X SDS Lysis Buffer at 24 hpi. A: Immunoblots of Nbs1 and Mre11 show no decrease in protein abundance during infection. B: Immunoblot of Rad50 shows no decrease in protein abundance during infection. Immunoblot of TAg shows LTA expression in infected samples. Mutants NG59 and 808A show lower levels of LTA than WT. As expected, only RA and NG59 infected samples show bands corresponding to mT. C, D, E: Quantification of Mre11, Rad50, and Nbs1 immunoblots normalized to their respective tubulin loading control followed by normalization to the UI sample confirms that there is not a decrease in protein accumulation during infection. F. Quantification of LTA and mT immunoblots normalized to a tubulin control shows lower levels of LTA in mutant viruses.

### Determination of Viral Titers via a Percent Infection Assay of RA, NG59, and 808A MPyVs

In order to understand the effects of viral protein expression on cell signaling, we attempted to infect cells with equal amounts of virus. The viral titer for MPyV RA was known to be  $1.8 \times 10^8$  PFU/ml. The titers of the mutant viruses were not previously known. Earlier work attempted to calculate the titers of MPyV mutants using viral plaque assays. However, the viral strains used in this study are known as ‘small plaque’ viruses and were not found to create any observable plaques by numerous staining method protocols. Hemagglutination (HA) assays were also performed with the MPyV strains. The drawback of this assay is that by binding to the viral capsid proteins, the HA assay only measures viral particles in a sample and does not report infectious particles (those with productive genomes). Estimations of viral particles/ml using this method may be 7-8 orders of

magnitude greater than the number of productive virions/ml in the stocks of each MPyV strain, indicating a large number of empty/non-productive virion capsids.

To overcome the issues that arise with other methods, Katie Heiser developed a new assay that can be used to measure the levels of infection between WT and mutant MPyV strains. With standard curves of infection levels, these values could be used to calculate relative viral titers for the mutant viruses. The levels of infection between WT and mutant MPyVs were compared via an immunofluorescence staining analysis of TAg and VP1 (Fig. 8). Using serial dilutions, a standard curve was generated for each virus that compared the percent of infection to the dilution of virus used. TAg expression was used as a marker of an infected cell and determined the calculations. Using the curve for each MPyV strain, the dilution was identified at which there was a 50% level of infection (# infected cells/total number of cells as quantified by expression of viral TAg). The dilution was then used to calculate for MPyV RA to comparatively calculate the viral titers of each mutant. Mutant NG59 has a titer of  $1.123 \times 10^7$  PFU/ml and mutant 808A has a titer of  $2.36 \times 10^7$  PFU/ml. With these titers, the same MOI can be used to infect cells which controls for levels of infection between the viruses. Images shown are the levels of infection achieved from the dilutions of virus used in the phospho-kinase array at an MOI equal to 30.

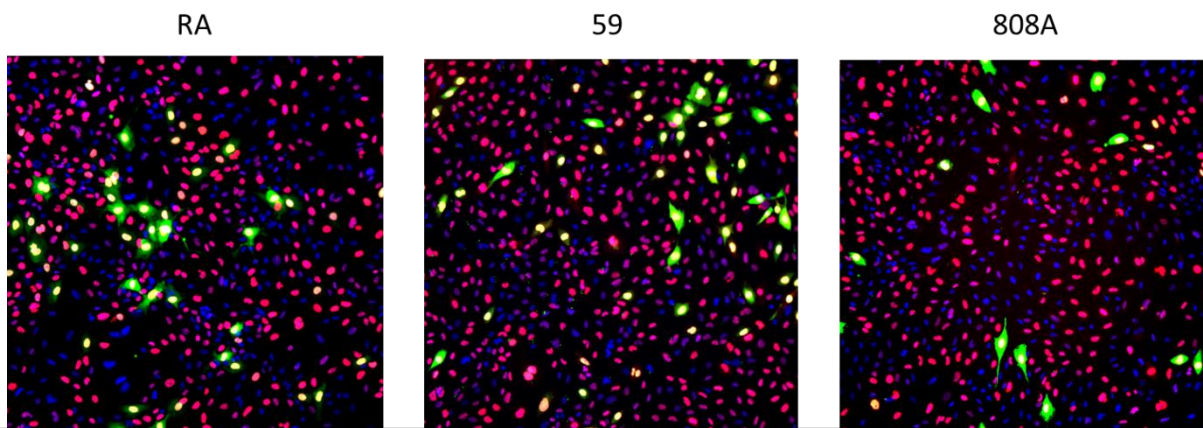


**Figure 8: Levels of Infection by WT MPyV and MPyV mutants NG59 and 808A for Array Data.** Each MPyV, RA, NG59, and 808A was diluted to an MOI of 30 for infection. At 26 hpi the cells were fixed, permeabilized, and stained for TAg (AlexaFluor 546) and VP1 (AlexaFluor 448). Nuclei are depicted in blue, TAg in red, and VP1 in green. Calculated levels of infection based on TAg expression averaged across 6 wells per virus were found to be: MPyV RA: 69.5%, mutant MPyV NG59: 79.6%, and mutant 808A MPyV: 49.3%. This and prior work has indicated that virus mutant 808A takes longer to infect and express viral proteins than MPyV RA or mutant NG59 and may not be able to reach the same peak levels of

**Akt S473 phosphorylation is induced during NG59RA infection**

Cell proliferation signaling via the Akt pathway can result in transition to S phase and promotion of vDNA replication. MPyV RA infection significantly increases phosphorylation of Akt ( $p=0.022$ ) (Fig. 9). This evidence suggests an effect between mTAg and Akt. The increase in

phosphorylation of Akt by mutant MPyV NG59 is also significant ( $p=0.0058$ ) (Fig. 9). This may suggest that mutant MPyV NG59 mTAg has partial functionality, allowing it to participate in Akt activation. There is no difference in activation of Akt by mutant

MPyV 808A (Fig. 9) which conveys that mTAg is essential for the activation of Akt.

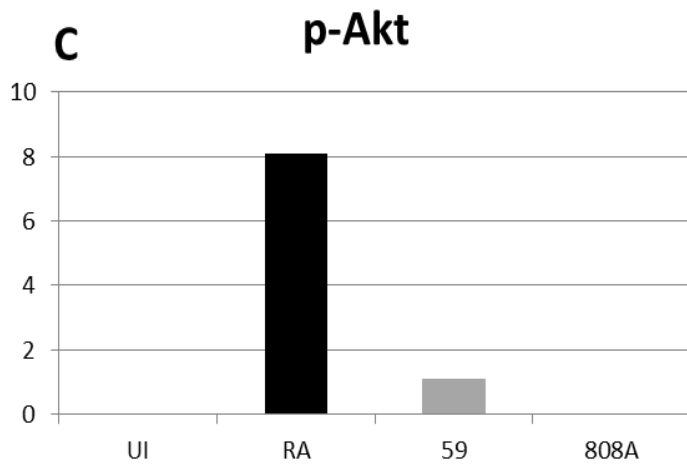
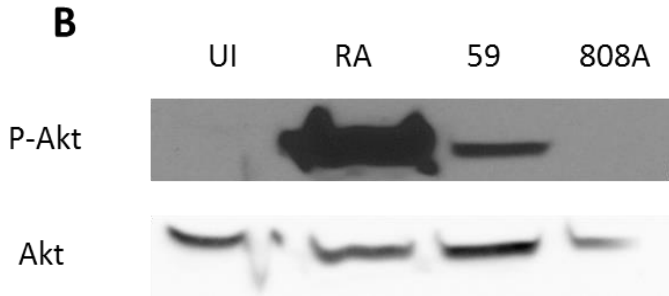
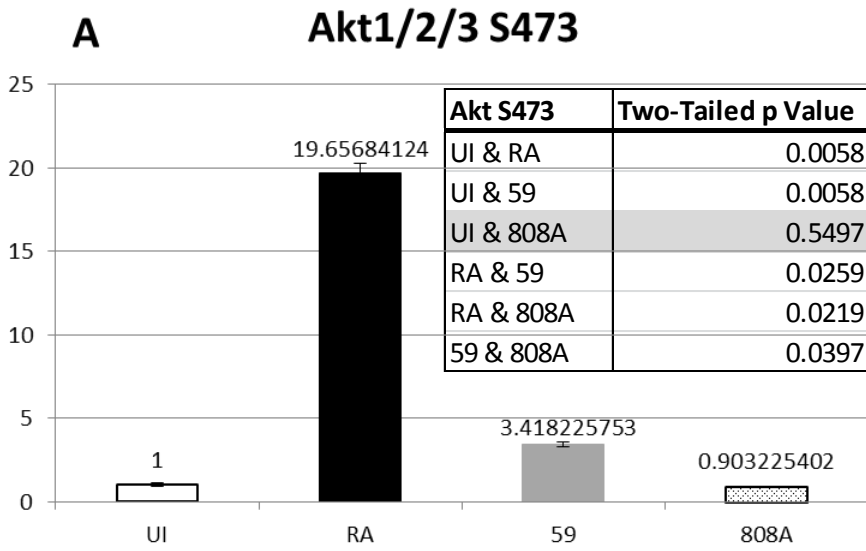


**Figure 9: Analysis of p-Akt levels during PyV infection.** A: Phospho-kinase array data displaying levels of phosphorylation on S473 of Akt during viral infection. B: Immunoblot data from the same lysate as the array experiment confirms that phosphorylation of Akt increased significantly during RA infection as compared to UI or mutant viruses. The antibody used for immunostaining has specificity for the same S473 site as the array antibody. C: Quantification of immunoblot from B as normalized to total Akt demonstrates the same trend as in A.

## TOR and PRAS40 phosphorylation is induced during MPyV infection

During infection, PRAS40 inactivation and subsequent TOR activation occurs at the highest levels in MPyV WT virus, though all viruses indicate >2x more phosphorylation of PRAS40 than uninfected cells (Fig. 10). The increased phosphorylation of PRAS40 by all viruses may indicate that LTag plays some role (either directly or indirectly) in directing phosphorylation of PRAS40 T246 than does mTAg or sTAg. However, the difference in phosphorylation of RA and both mutant viruses of ~35.7% is statistically significant (Fig. 10), implying that mTAg also directly targets PRAS40. TOR activation in the presence of mTAg shows a similar pattern as does the removal of its inhibitor, PRAS40, with ~33.3% greater activation in the presence of MPyV RA than the two mutant viruses (Fig. 10).

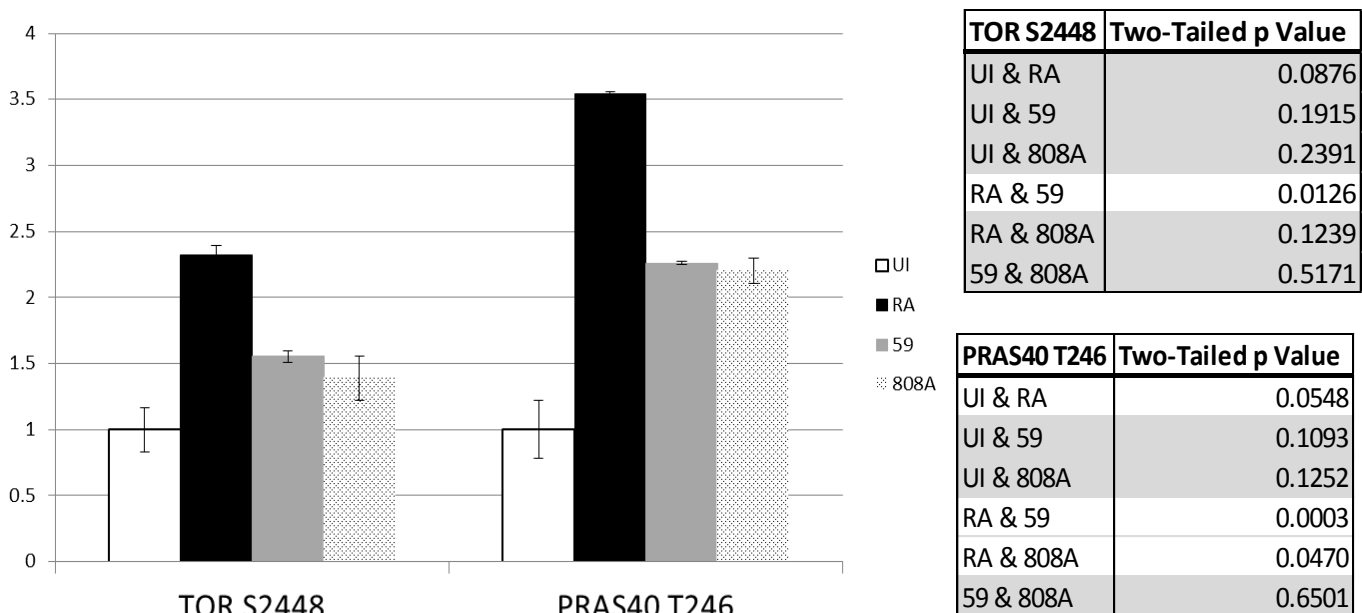
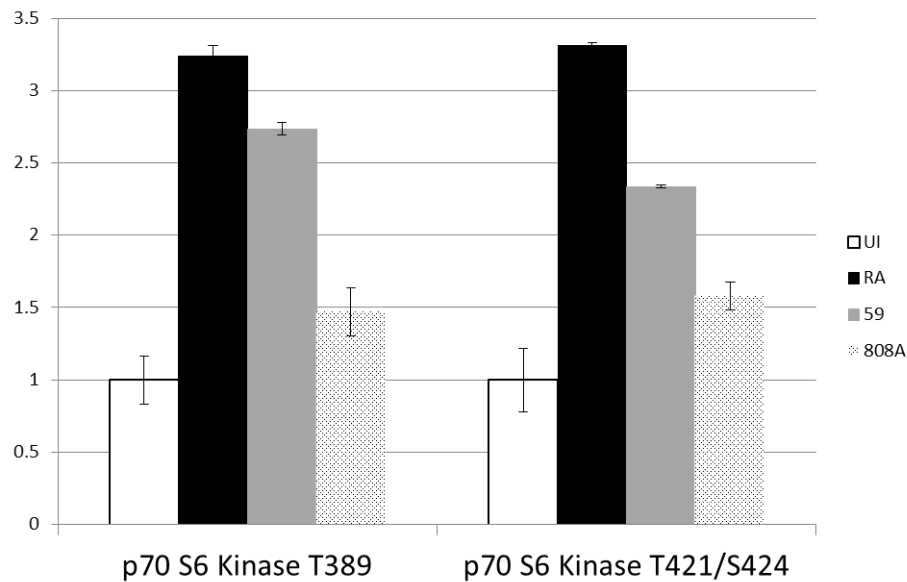


**Figure 10: Downstream effectors TOR S2448 and PRAS40 T246 phosphorylated by Akt from phospho-kinase array data.** PRAS40 T246 phosphorylation increases due to infection by MPyVs RA, NG59, and 808A. The result is activation of the TOR complex due to relief from the inhibitory effects of PRAS40. The most significant increase occurs in MPyV RA, suggesting that mTAg mediates this phosphorylation event; however, the slight increase in phosphorylation by both mutant viruses may indicate that LTag has either a direct or indirect role in activating TOR through PRAS40. TOR S2448 phosphorylation occurs in a nearly identical pattern as does PRAS40.

## P70 S6 Kinase phosphorylation is induced during infection with NG59RA, NG59, and 808A viruses

MPyV RA induces ~69.2% more phosphorylation of p70 S6 Kinase when compared to an UI sample (Fig 11). The mutant MPyV NG59 lysate induces ~33.3-45.5% additional phosphorylation at the three sites (T389, T421, S424) than the mutant MPyV 808A sample, but both mutants phosphorylate this protein at lower levels than does WT MPyV (Fig. 11). This data may indicate that the NG59 mutant virus has some partial mTAg functionality and contributes to phosphorylation of p70 S6 Kinase T389. It is also possible that expression of LTA<sub>g</sub> is either directly or indirectly affecting phosphorylation of these sites.



p70 S6 Kinase T389	Two-Tailed p Value	p70 S6 Kinase T421, S424	Two-Tailed p Value
UI & RA	0.0069	UI & RA	0.0741
UI & 59	0.0448	UI & 59	0.1067
UI & 808A	0.1815	UI & 808A	0.0297
RA & 59	0.1837	RA & 59	0.1019
RA & 808A	0.0193	RA & 808A	0.0986
59 & 808A	0.1028	59 & 808A	0.1847

**Figure 11: p70 S6 Kinase activation via phosphorylation in response to PyV infection.**

Phosphorylation of p70 S6 Kinase T389, T421, and T424 residues increases due to infection by MPyV. WT MPyV has the greatest effect in promoting phosphorylation, indicating the importance of functional mTAg.

### A lack of phosphorylation of p27 is observed during infection with NG59RA, NG59, and 808A viruses

There is a 5.4-fold reduction in phosphorylation on the T198 residue of p27 during infection of MPyV RA (Fig. 12). The mutant MPyVs NG59 and 808A also show reductions in phosphorylation between one and two-fold (Fig. 12). These results suggest that the presence of MPyV encourages the cell cycle to progress to S phase by interacting either directly or indirectly with p27. mTAg has a pronounced effect on this outcome, however there may be influence from LTA<sub>g</sub> either through direct or indirect mechanisms.

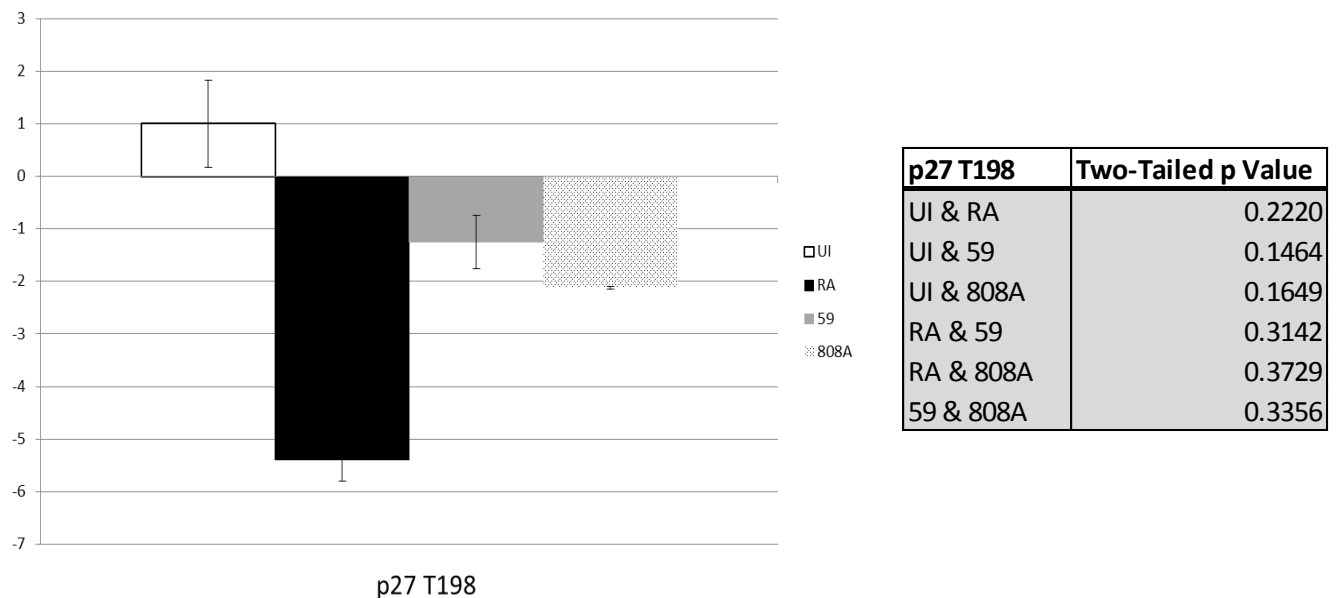


**Figure 12: p27 phosphorylation is reduced during MPyV infection.** The data shown here indicate that phosphorylation of p27 is reduced during MPyV infection. The presence of mTAg seems to significantly affect this outcome; however, because the mutant MPyVs also show reduced phosphorylation, a direct or indirect role for LTA<sub>g</sub> should also be considered.

## VI. Discussion

Previous work has indirectly implicated MPyV mTAg in affecting major cell cycle signaling pathways, yet these studies were done either by transfection of mTAg plasmids or through the use of primate PyV SV40. Here I show cell signaling dysregulation in accordance with previously published work during normal infection conditions by MPyV.

PyV initiated DDR via TAg expression has been previously established as a hallmark of infection that keeps the cell in S phase to promote viral replication (An et. al. 2012). Contrary to the studies of SV40 TAgS by Zhao et. al. 2008, we found no evidence that supports a decrease in abundance of MRN during MPyV infection. SV40 LTAg has been shown to bind Nbs1, yet a similar interaction in MPyV is unclear, and does not target the complex for degradation (Wu et. al. 2004). Mre11 and vDNA have been shown to co-localize during MPyV infection, suggesting that the virus does in some way modify the ATM DDR pathway (Erickson et. al. 2012). Activation of ATM and a subsequent pause in the cell cycle is advantageous for PyV because this prevents the cell from moving out of S phase. The activation states of other ATM pathway proteins were considered in the context of infection. Antibodies for p-ATM, p-Nbs1, and  $\gamma$ H2AX were used in immunostaining but did not give results in our MEF system. Furthermore, p-ATM is a large protein of 370<sup>+</sup> kDa and difficult to resolve on a gel. Commercial antibodies for other phosphorylated MRN and DDR proteins are not currently available for use in MEFs.

Under the premise that MPyV most efficiently replicates when the cell is in S phase, we began preliminary work into understanding how the virus, specifically TAg splice variants, might affect the activation states of proteins involved in cell cycle signaling and cell proliferation pathways. Such interactions with cell cycle regulators could potentially lead to cellular transformation and tumor formation. The phospho-kinase array developed by R&D Systems provided an efficient tool for such a study.

Investigations by Summers et. al. 1998 and Meili et. al. 1998 both established that MPyV mTAg is involved in the activation of Akt and p70 S6 Kinase, dependent on the simultaneous stimulation of PI3K. Summers et. al. describes how mTAg can facilitate these interactions by comparing the intracellular domain of mTAg to that of cytoplasmic tails of activated growth factor receptors which interact with a plethora of signaling molecules to regulate numerous downstream effects. The phospho-kinase array establishes a nineteen-fold increase in phosphorylation of Akt S473 and a greater than three-fold increase in phosphorylation of p70 S6 Kinase T389, T421, and T424 during MPyV RA infection as compared to UI cells. The mutants analyzed in this array contained either functionally handicapped mTAg (NG59) or were completely missing mTAg (808A), and thus did not show the same levels of activation as did WT virus (RA). The previously published studies looked at the ability of mTAg mutants to bind p85 and thus activate PI3K through the use of transfected mTAg mutants rather than under the conditions of normal infection (i.e. simultaneous expression of LTAg) (Summers et. al. 1998 and Meili et. al. 1998). It is promising that in the context of a full infection where LTAg is expressed, we have data to support mTAg as the primary contributor to Akt and p70 S6 Kinase activation.

Signaling by TOR and p70 S6 Kinase promotes cell proliferation and translation initiation which is necessary for the virus to produce high quantities of viral packaging proteins VP1/2/3. p70 S6 Kinase is a direct target of the activated TOR complex. However, TOR cannot be activated until inhibitor molecule PRAS40 dissociates. Activated Akt serves as the kinase that facilitates transfer of a phosphate group to PRAS40 T246 which removes its inhibitory effect on TOR. Furthermore, TOR S2448 and p70 S6 Kinase have been found to phosphorylate each other in order to respond to contrary cellular signals. Some of these signals include DDR response via ATM (Sancak et. al. 2007, Watanabe et. al. 2011). Given that PRAS40, TOR, and p70 S6 Kinase are direct downstream effectors of Akt and that they are intimately related functionally, it makes sense that

their levels of phosphorylation would have similar patterns under infection by MPyV. Additionally, the important role of mTAg in activating these pathways is directly linked to activation of Akt which initiates all of these downstream effects. Moreover, it becomes increasingly apparent that the MPyV mutant NG59 may have retained partial functionality due to the higher levels of activation observed as compared to infection by mutant 808A. Though the p-values between mutant NG59 and mutant 808A are not statistically significant for these proteins, they may be biologically significant and could become statistically significant if greater than two replicates are considered.

p27 is another example of what appears to be a biologically significant trend that is not calculated as statistically significant within two replicates. Control of the cell cycle is tightly regulated under normal conditions. It is interesting that during infection of MPyV RA, there is a five-fold reduction in phosphorylation of p27 as compared to an uninfected sample. The virus must either directly or indirectly be affecting the activation state of p27 to promote cell cycle progression to S phase. Data for the activation state of RSK shown in the appendix indicates that RSK is activated in the presence of MPyV RA and NG59. Evidence from Larrea et. al. 2009 has shown that RSK can phosphorylate p27 at T198 which mislocalizes p27 from the nucleus to the cytoplasm. Additionally, PI3K, which is known to be activated in the presence of PyV can contribute to mislocalization of p27. This activation of p27 directly leads to increased cell motility which is related to metastatic activity in the context of cancer cells (Larrea et. al. 2009).

SV40 sTAg (analogous to MPyV mTAg) has been characterized by its propensity for binding PP2A. SV40 sTAg has an inhibitory effect on PP2A which results in loss of its phosphatase activity. There is evidence for SV40 sTAg, together with PP2A actively working to reduce p27 and its hold on the cell cycle (Schuchner S. and Wintersberger 1999). This data was obtained via transfection of plasmids containing PyV sTAg. Here I have established a pattern that mimics these results during full infection by MPyV. MPyV RA, expressing mTAg as normal, saw the largest reduction in

phosphorylation of p27 as would be expected. Furthermore, knowledge of MPyV mTAg interaction with PP2A to promote cellular transformation via disruption of the cell cycle indicates that the virus collaborates with this phosphatase to execute the effects observed on p27. Repeated observations of the phosphorylation levels of p27 would be beneficial in solidifying conclusions made about the interaction between viral TAgS and the p27 protein.

This study highlights the importance of studying MPyV TAgS and their effects on the cell independently of SV40 TAgS. While structurally similar, evidence for TAgS from the two viruses seems to show that they may differ somewhat in carrying out their functions. More work is needed to comprehend the complex interactions that the viruses have on cell signaling proteins that support efficient viral replication. Additional data from the phospho-kinase array implicates other fundamental signaling pathways such as ERK/MAPK, JAK/STAT, and interactions with p53. Follow-up investigations with the MPyV mutant NG18 which produces a truncated and functionally deficient mTAg transcript and no sTAg transcript would be prudent to further elucidate the influence of TAgS on these processes and pathways.

VII. Appendix

Figure A1: Complete Phospho-Kinase Array Data

All phospho-targets represented here were produced in the same manner as the ones discussed previously. These data are interesting, but have yet to be thoroughly analyzed.

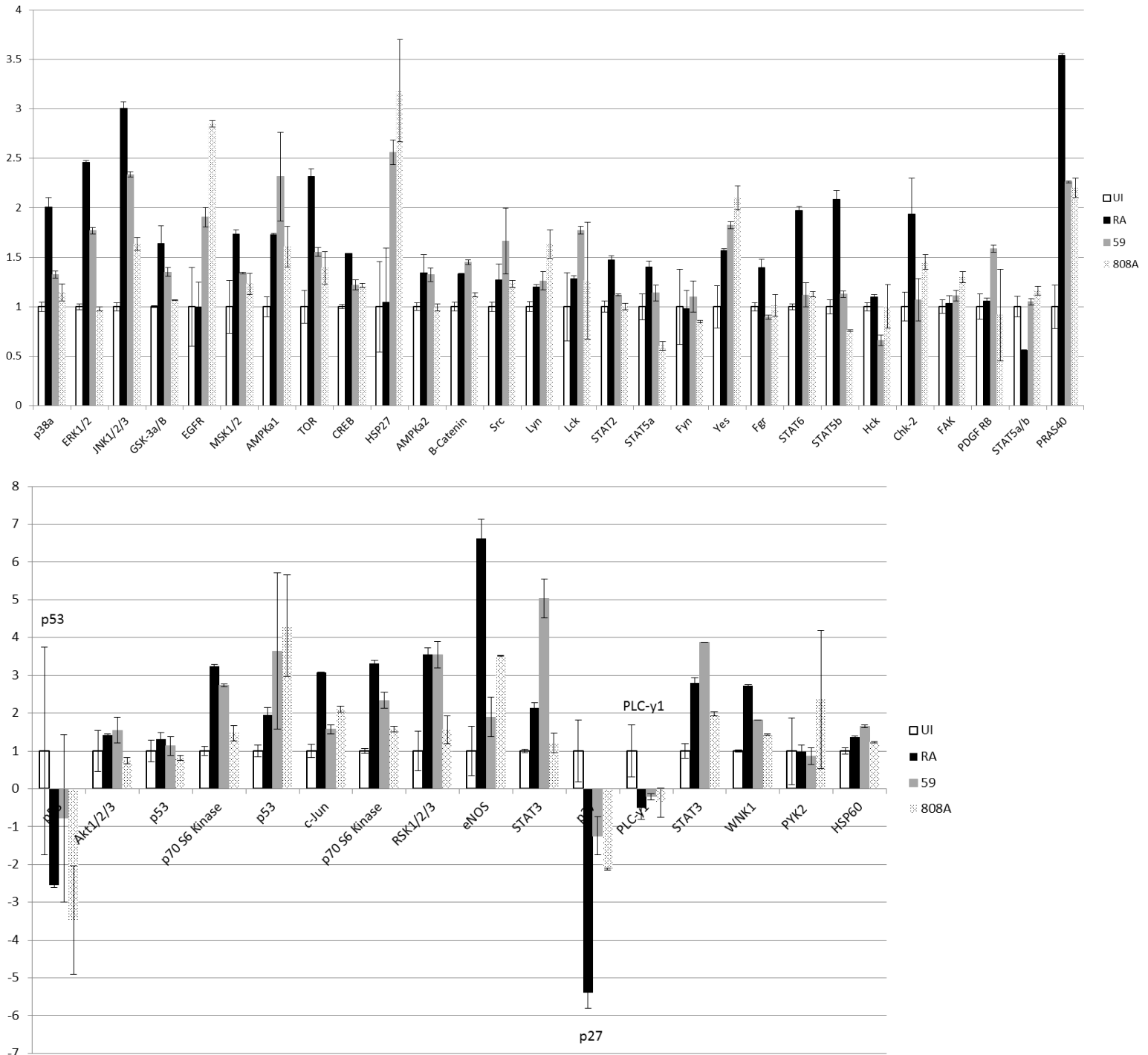
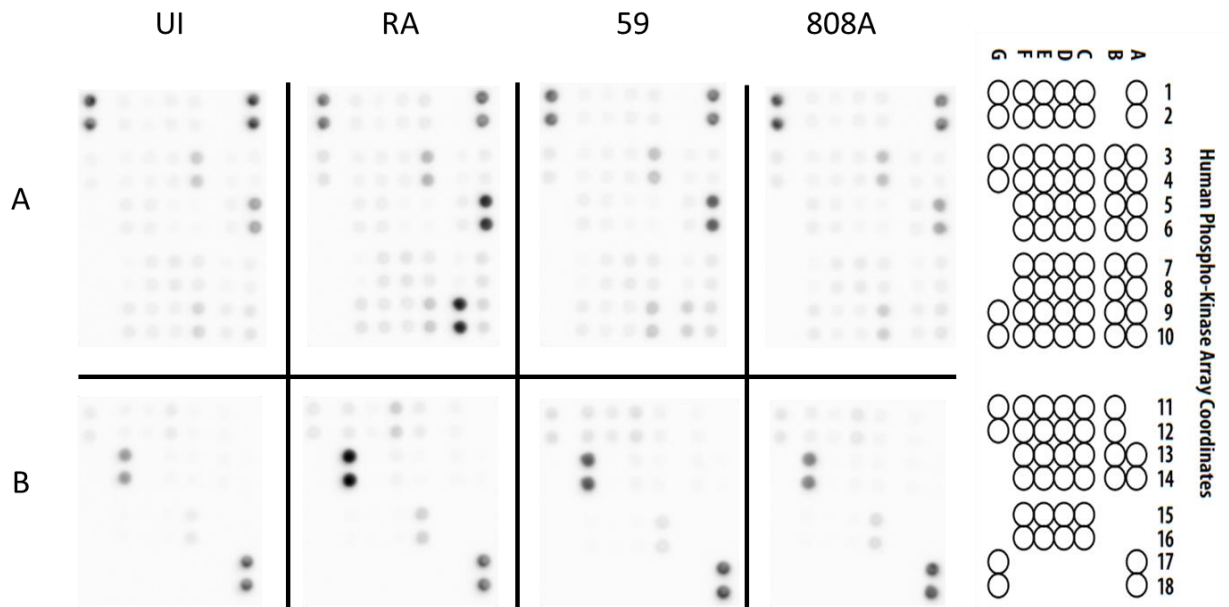


**Figure A2: Phospho-Kinase Array Membranes and Antibody Location Key**

The key to the membranes from the R&D Phospho-kinase array depicts the dots and assigns them a specific coordinate. Each dot then corresponds to the antibody for a particular protein as listed below. Additionally, the coordinate at which a particular phosphorylation mark is assessed is noted. Some proteins were repeated in the assay with different phosphorylation marks (e.g. Akt, p70 S6 Kinase, p53, etc.). There are two distinct dots per protein and phosphorylation mark.



Membrane/ Coordinate	Target/Control	Phosphorylation Site	Membrane/ Coordinate	Target/Control	Phosphorylation Site
A-A1, A2	Reference Spot	—	A-E1, E2	Fyn	Y420
A-A3, A4	p38a	T180/Y182	A-E3, E4	Yes	Y426
A-A5, A6	ERK1/2	T202/Y204, T185/ Y187	A-E5, E6	Fgr	Y412
A-A7, A8	JNK 1/2/3	T183/Y185, T221/ Y223	A-E7, E8	STAT6	Y641
A-A9, A10	GSK-3a/ $\beta$	S21/S9	A-E9, E10	STAT5b	Y699
B-A13, A14	p53	S392	B-E11, E12	STAT3	Y705
B-A17, A18	Reference Spot	—	B-E13, E14	p27	T198
A-B3, B4	EGF R	Y1086	B-E15, E16	PLC- $\gamma$ 1	Y783
A-B5, B6	MSK1/2	S376/S360	A-F1, F2	Hck	Y411
A-B7, B8	AMPK $\alpha$ 1	T183	A-F3, F4	Chk-2	T68
A-B9, B10	Akt 1/2/3	S473	A-F5, F6	FAK	Y397
B-B11, B12	Akt 1/2/3	T308	A-F7, F8	PDGF R $\beta$	Y751
B-B13, B14	p53	S46	A-F9, F10	STAT5a/b	Y694/Y699
A-C1, C2	TOR	S2448	B-F11, F12	STAT3	S727
A-C3, C4	CREB	S133	B-F13, F14	WNK1	T60
A-C5, C6	HSP27	S78/S82	B-F15, F16	PYK2	Y402
A-C7, C8	AMPK $\alpha$ 2	T172	A-G1, G2	Reference Spot	—
A-C9, C10	$\beta$ -Catenin	—	A-G3, G4	PRAS40	T246
B-C11, C12	p70 S6 Kinase	T389	A-G9, G10	PBS (Negative Control)	—
B-C13, C14	p53	S15	B-G11, G12	HSP60	—
B-C15, C16	c-Jun	S63	B-G17, G18	PBS (Negative Control)	—
A-D1, D2	Src	Y419			
A-D3, D4	Lyn	Y397			
A-D5, D6	Lck	Y394			
A-D7, D8	STAT2	Y689			
A-D9, D10	STAT5a	Y694			
B-D11, D12	p70 S6 Kinase	T421/S424			
B-D13, D14	RSK1/2/3	S380/S386/S377			
B-D15, D16	eNOS	S1177			

### **VIII. Acknowledgments**

I would like to thank the entire Garcea lab for their support during this process. First, I would like to thank Dr. Bob Garcea for allowing me the wonderful opportunity to join the lab and participate in this research as well as encouraging and guiding me throughout the project. I would also like to thank Dr. Kim Erickson for showing me the ways of the lab and mentoring me day-to-day as I ran into tough technical spots. Special thanks goes to Katie Heiser and Sam O'Hara for spending many late nights in the lab with me, helping me with all of my microscopy, answering my ceaseless questions, and challenging me to think critically about science. I could not have finished this project without their scientific and emotional support. Thanks to Natalie Meinerz for all of the treats that appeared at lab meetings and for keeping the lab fun☺. Thanks to my committee members Dr. Christy Fillman, Dr. Jim Goodrich, and Dr. Dylan Taatjes for their time and assistance with my thesis defense.

## IX. References

- An P, et. al. (2012) Large T Antigens of Polyomaviruses: Amazing Molecular Machines. Annual Review of Microbiology. (66), 213–36.
- Carmichael G. and Benjamin T. (1979) Identification of DNA Sequence Changes Leading to Loss of Transforming Ability in Polyoma Virus. *Journal of Biological Chemistry*. 255(1), 230-235.
- Dahl J. et. al. (2005) Induction and Utilization of an ATM Signaling Pathway by Polyomavirus. *Virology*. 79(20), 13007-13017.
- Das D. and Imperiale M. "Transformation by Polyomaviruses." *DNA Tumor Viruses*. Ed. James Pippas and Blossom Damania. Springer US. 2009. 53-74. PDF File.
- Dawei Li, et. al. (2009) Structure of the replicative helicase of the oncoprotein SV40 large tumour antigen. *Nature*. (423), 512-518.
- Diaz-Moralli S. et. Al. (2013). Targeting cell cycle regulation in cancer therapy. *Pharmacology & Therapeutics*. (138), 255-271.
- Dilworth S. (2002) Polyoma virus middle T antigen and its role in identifying cancer-related molecules. *Nature Reviews Cancer*. 2(12), 951-6.
- Erickson K. et. Al. (2012) Virion Assembly Factories in the Nucleus of Polyomavirus-Infected Cells. *PLOS Pathogens*. 8(4) e1002630.
- Fanning Ellen, Xiaorong Zhao, Xiaohua Jiang. *DNA Tumor Viruses*. Chapter 1. New York. Springer Science+Business Media. 2009. Print.
- Fluck M and Schaffhausen B. (2009) Lessons in Signaling and Tumorigenesis from Polyomavirus Middle T Antigen. *Microbiology and Molecular Biology Reviews*. 73(3), 542-563.
- Fujita N. et. Al. (2003) Phosphorylation of p27Kip1 at Threonine 198 by p90 Ribosomal Protein S6 Kinases Promotes Its Binding to 14-3-3 and Cytoplasmic Localization. *The Journal of Biological Chemistry*. 278(49), 49254–49260.

- Garcea Robert L et. al. (1989) Separation of Host Range from Transformation Functions of the hr-t Gene of Polyomavirus. *Virology*. (168), 312-319.
- Hwang J, et. al. (2013) Protein phosphatase 2A isoforms utilizing A $\beta$  scaffolds regulate differentiation through control of Akt protein. *J Biol Chem*. 288(44), 32064-73.
- Kean J. and Garcea R. "Polyomaviruses and Disease." *DNA Tumor Viruses*. Ed. James Pippas and Blossom Damania. Springer US. 2009. 53-74. PDF File.
- Kurz Ebba U, Lees-Miller Susan P. (2004) DNA damage-induced activation of ATM and ATM-dependent signaling pathways. *DNA Repair*. (3), 889–900.
- Larrea M. et. Al. (2009) RSK1 drives p27Kip1 phosphorylation at T198 to promote RhoA inhibition and increase cell motility. (106)23, 9268–9273.
- Meili R, et. al. (1998) Protein kinase B/Akt is activated by polyomavirus middle-T antigen via a phosphatidylinositol 3-kinase-dependent mechanism. *Oncogene*. 19;16(7), 903-7.
- Sancak Y. et. Al. (2007) PRAS40 Is an Insulin-Regulated Inhibitor of the mTORC1 Protein Kinase. *Molecular Cell*. (25), 903–915.
- Schuchner S. and Wintersberger E. (1999) Binding of Polyomavirus Small T Antigen to Protein Phosphatase 2A Is Required for Elimination of p27 and Support of S-Phase Induction in Concert with Large T Antigen. *Journal of Virology*. (73)11, 9266–9273.
- Summers S, et. al. (1998) Polyoma middle T antigen activates the Ser/Thr kinase Akt in a PI3-kinase-dependent manner. *Biochemical and Biophysical Research Communications*. 246(1), 76-81.
- Watanabe R. et. Al. (2011) mTOR Signaling, Function, Novel Inhibitors, and Therapeutic Targets. *The Journal of Nuclear Medicine*. 52(4), 497-500.
- Wiza C, et. al. (2012) Role of PRAS40 in Akt and mTOR signaling in health and disease. *Am J Physiol Endocrinol Metab*. (302)12, E1453-60.

Wu, X., D. Avni, T. Chiba, F. Yan, Q. Zhao, Y. Lin, H. Heng, and D. Livingston. (2004) SV40 T antigen interacts with Nbs1 to disrupt DNA replication control. *Genes Dev.* (18), 1305–1316.

Zhao X, et al. (2008) Ataxia telangiectasia-mutated damage-signaling kinase- and proteasome-dependent destruction of Mre11-Rad50-Nbs1 subunits in Simian virus 40-infected primate cells. *J Virol* (82), 5316–5328.